JACC Vol. 19, No. 2
February 1992:450–7

Mechanical Correlates of the Third Heart Sound

DONALD D. GLOWER, MD, ROBERT L. MURRAH, MD, CRAIG O. OLSEN, MD, JAMES W. DAVIS, MSEE, J. SCOTT RANKIN, MD

Durham, North Carolina

In seven chronically instrumented conscious dogs, micromanometers measured left ventricular pressure, and ultrasonic dimension transducers measured left ventricular minor-axis diameter; the latter recording was filtered to examine data between 20 and 100 Hz. Acceptable external heart sounds were recorded with a phonocardiographic microphone in four of the seven dogs. With each dog sedated, intubated and mechanically ventilated, data were obtained during hemodynamic alterations produced by volume loading, phenylephrine, calcium infusion and vena caval occlusion.

Damped oscillations were noted consistently in the left ventricular diameter waveform toward the end of rapid ventricular filling. These wall vibrations, assessed by the filtered diameter, correlated well with the third heart sound (S_3) on the phonocardiogram. The peak frequency of the wall vibrations increased with increased diastolic pressure ($p = 0.004$), probably reflecting an increase in myocardial wall stiffness. In contrast, the amplitude of the vibrations varied directly with left ventricular filling rate ($p = 0.0001$).

Thus, S_3 seemed to be related specifically to ventricular wall vibrations during rapid filling, and the spectra of the amplitude-frequency relation shifted toward the audible range with increases in diastolic pressure, wall stiffness or filling rate. Spectral analysis of S_3 may be useful in assessing pathologic changes in myocardial wall properties.

(J Am Coll Cardiol 1992;19:450–7)

Since the appearance of Charles Potain's classic essay in 1900 (1) describing the third heart sound (S_3), scientific controversy has existed over its biologic mechanisms and the associated hemodynamic and pathologic implications. Three principal theories of origin attribute S_3 to 1) valvular and subvalvular phenomena (2–5), 2) the impact of the heart against the chest wall (6–8), and 3) ventricular wall vibrations (9–16). Most investigators (9–16) now accept ventricular wall vibrations as the origin of S_3. The following studies were designed to investigate the mechanical basis of S_3 in an intact animal model and to examine the physiologic factors that modify the characteristics of S_3. Specifically, the questions to be examined were 1) does the energy transmitted to the ventricular wall during rapid filling contribute to the amplitude of S_3, and 2) does the frequency content of S_3 behave according to set physical principles governing the oscillation of viscoelastic materials.

From the Departments of Surgery and Biomedical Engineering, Duke University Medical Center, Durham, North Carolina. This study was supported in part by Grants HL-09315 and HL-29436 and SCOR Grant HL-17670 from the National Heart, Lung, and Blood Institute, National Institutes of Health, Bethesda, Maryland. Dr. Glower is recipient of the John F. Gibbon Jr. Research Scholarship of The American Association for Thoracic Surgery, Manchester, Massachusetts.

Manuscript received May 1, 1991; revised manuscript received July 3, 1991, accepted July 24, 1991.

Address for reprints: Donald D. Glower, MD, Box 3851, Duke University Medical Center, Durham, North Carolina 27710.

Methods

Experimental preparation. Seven healthy adult mongrel dogs (18 to 24 kg) were surgically instrumented for subsequent studies in the closed chest state. Each dog was anesthetized with intravenous thiamylal sodium (25-mg/kg body weight) and ventilated with a volume respirator. A left thoracotomy was performed through the fifth intercostal space by sterile technique, and epicardial ultrasonic dimension transducers (17) were positioned across the left ventricular anterior-posterior minor axis to measure left ventricular diameter and ventricular wall oscillations (Fig. 1). During the procedure, silicone rubber pneumatic occluders were positioned around the inferior vena cava and descending thoracic aorta. A silicone rubber tube was implanted in the base of the left atrium, and a second rubber tube was left in the pleural space for later passage of micromanometers. The pericardium was left widely open, the transducer leads and silicone tubes were exteriorized through subcutaneous tunnels dorsal to the thoracotomy, and the incision was repaired in multiple layers. All dogs received daily intramuscular injections of procaine penicillin-G (2×10^5 U) and dihydrostreptomycin (250 mg), along with a single injection of ferric hydroxide (100 mg).

At the time of study, the dimension transducers were coupled directly to a modified, dual output sonomicrometer that sampled data at a rate of 1,000 samples/s. One channel interposed a two-pole filter to produce a 12-db/octave attenuation above 100 Hz yielding an effective frequency response of 0 to 50 Hz. This channel was used to monitor gross

0735-1097/92/$5.00

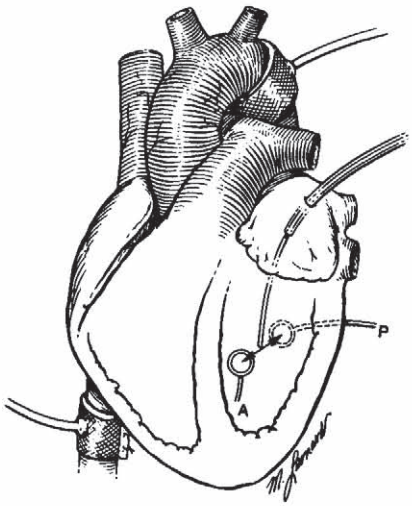

Figure 1. The standard preparation employed in this study with ultrasonic transducers positioned across the minor-axis diameter of the left ventricle and inferior vena cava and descending thoracic aorta pneumatic occluders. A solid state pressure transducer was passed into the left ventricle through the implanted left atrial tube. A and P = anterior and posterior left ventricular dimension transducers, respectively.

cardiac dimensions with a resolution of approximately 0.05 mm. The second channel interposed a 5-Hz high pass filter to remove the gross minor-axis diameter waveform, followed by two sequential bandpass filters to select frequencies between 20 and 100 Hz (Fig. 2). All filters were the Butterworth type to minimize ringing, and a minimal number of poles was used to provide a sufficient slope of attenuation outside the desired bandpass (18).

Left ventricular and pleural pressure measurements were obtained with micromanometers (PC-350, Millar Instruments) coupled to pressure amplifiers (8805-C, Hewlett-Packard). Manometers were passed into the mid-left ventricle and pleural space to yield left ventricular transmural pressure as the difference between left ventricular and pleural pressures. In four of the seven dogs external phonocardiograms of acceptable quality were obtained on the chest wall overlying the ventricular apex with use of a standard amplification system and an Elema-Scholander microphone (EMT-25B).

Figure 2. Digital examples of the minor-axis diameter signal after filtering with the 50-Hz low pass filter (**middle panel**) and with the 20- to 100-Hz bandpass filter (**lower panel**). The **top panel** shows the derivative of minor-axis diameter (dD/dt) used to determine the rapid filling phase (see text).

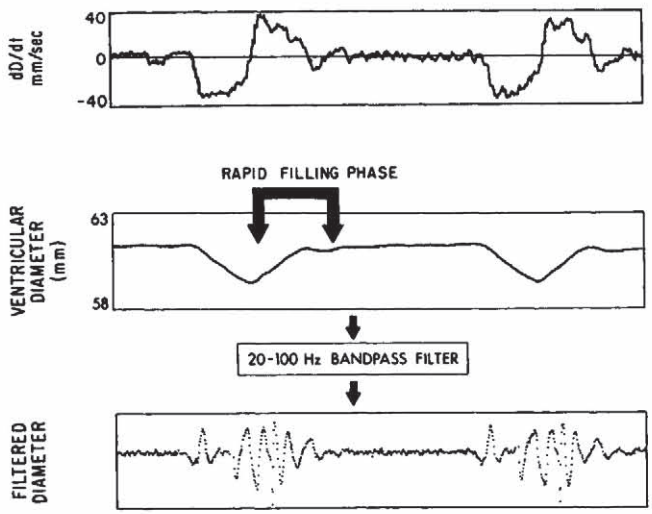

Physiologic protocol. After recovery from implantation (7 to 10 days), each dog was anesthetized (intravenous morphine sulfate, 0.5 to 1 mg/kg), intubated and ventilated at a minute volume of 6 liters. The ventilator was disconnected, and data were recorded during brief periods of apnea with the animal paralyzed and the endotracheal tube open to air. Apnea eliminated respiratory variations in filling rate and pressure, standardized the physiologic data from beat to beat and minimized extraneous breath sounds. Bradycardia was maintained by administration of propranolol (1 to 5 mg) to permit analysis of a sufficient number of digital data points during rapid diastolic filling to achieve 2- to 3-Hz resolution with a Fourier analysis program developed in our laboratory. All analog data were recorded on magnetic tape (model A, Vetter) for subsequent digital analysis. Filling rate was assessed by the derivative of minor-axis diameter (dD/dt) (19–22), and mean filling rate was defined as the average rate of change of minor-axis diameter during the rapid filling phase of diastole.

To facilitate Fourier analysis of third heart sound data, the rapid filling phase of diastole was defined as the period from peak positive dD/dt to 100 ms after the first subsequent zero crossing of dD/dt (Fig. 2). From each study, segments of steady state data were selected during baseline conditions, then during steady state control conditions of increased left ventricular end-diastolic pressure achieved by simultaneous blood volume expansion, infusion of phenylephrine (25 μg/kg per min intravenously), and partial descending thoracic aortic occlusion. These interventions routinely achieved left ventricular end-diastolic pressures of 20 to 40 mm Hg. Next, with the volume expansion, phenylephrine infusion and partial aortic occlusion still present, data were acquired during partial inferior vena cava occlusion to reduce ventricular diastolic pressure and diameter. Finally, data were recorded after a calcium infusion (15 mg/kg intravenously) that increased cardiac output and filling rate while minimally changing other variables. All studies were conducted in accordance with the Position of the American Heart Association on Research Animal Use.

Data analysis. Relevant data were analyzed for six cardiac cycles at each steady state, and the filtered dimension signals were averaged with use of a Fourier analysis program modified for this purpose. The resulting spectral analysis yielded calculated mean frequencies and mean amplitudes of wall vibrations that were representative of the events occurring during a given rapid diastolic filling period for each hemodynamic steady state. Multivariate linear regression

JACC Vol. 19, No. 2
February 1992:450–7

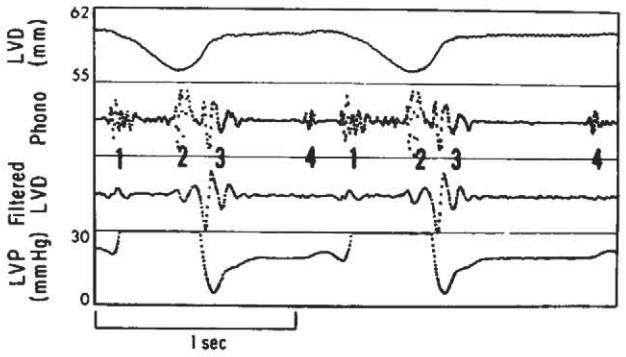

Figure 3. Representative raw digital recordings of left ventricular diameter (LVD), phonocardiogram (Phono), filtered diameter and left ventricular pressure (LVP) obtained during blood volume expansion, phenylephrine infusion and partial occlusion of the descending thoracic aorta. The fine oscillations on the unfiltered diameter signal were due to aliasing of the sonomicrometer sampling rate and analog to digital converter sampling rate; these frequencies were well beyond the physiologic range and were eliminated by the filtering procedures. All four heart sounds (1 to 4) are demonstrated on the phonocardiogram. A marked similarity was observed between the waveforms of S_3 on the phonocardiogram and the filtered ventricular wall oscillations during rapid filling.

analysis was used to detect relations between vibratory amplitude or frequency and the independent variables of left ventricular end-diastolic diameter, systolic and diastolic left ventricular pressures and mean rapid filling rate. The effects of vena caval occlusion or calcium infusion on individual variables were tested by analysis of covariance.

Results

Demonstration of S_3. After bandpass filtering of the raw minor-axis diameter signal in the volume-loaded state, the oscillations of the left ventricular wall during the rapid filling phase of diastole became readily apparent (Fig. 2). All four heart sounds were discerned in the four dogs with an acceptable phonocardiogram. Although there was limited correlation between the filtered diameter and the phonocardiogram for the first, second and fourth heart sounds, a striking similarity was evident between the waveform and temporal relations of ventricular wall vibrations during rapid filling and the phonocardiographic S_3 (Fig. 3).

Volume loading, phenylephrine infusion and partial occlusion of the descending thoracic aorta produced abnormally high left ventricular diastolic pressures (Table 1). The third heart sound was not present on the phonocardiogram in the control state, and it became apparent only after left ventricular diastolic pressure was increased by the loading interventions. Inferior vena cava occlusion decreased the minimal diastolic pressure and end-diastolic pressure ($p < 0.05$) (Table 1), whereas the rate of ventricular filling (as evidenced by the slope of the minor-axis dimension curve during rapid filling) remained essentially unchanged (Fig. 4). The decrease in ventricular filling pressure was accompanied

Table 1. Data in the Seven Study Dogs

Dog	End-Diastolic Diameter (mm)			Peak Systolic Pressure (mm Hg)			Minimal Diastolic Pressure (mm Hg)			End-Diastolic Pressure (mm Hg)			Mean Rapid Filling Rate (cm/s)			Ventricular Wall Vibrations					
																Mean Relative Amplitude			Mean Frequency (Hz)		
	A	B	C	A	B	C	A	B	C	A	B	C	A	B	C	A	B	C	A	B	C
1	32.1	35.3	35.3	150	151.1	169.4	6.4	9.4	10.8	11.5	16.3	28.1	1.24	2.21	3.44	0.889	0.947	1.216	10.28	10.83	11.37
2	65	65.6	65.6	>220	>220	>220	5.6	6.6	10.4	19	30.4	33.8	1.62	2	2.8	0.991	1.221	1.879	19.29	20.11	21.32
3	59	59	60.6	180.4	148.5	219.3	9.6	11.9	12.1	23.7	26.9	29.1	3.49	3.76	6.57	0.611	0.62	0.776	16.34	17.06	17.85
4	59.4	58.9	60.7	158.3	183.2	>220	10.9	14.1	20.5	18.6	28.9	38.7	2.13	2.91	3.8	1.155	1.579	1.623	18.81	20.92	25.05
5	58.7	60.7	60.4	200.3	208.5	200.1	4.9	12.5	8.9	15.5	27.5	20.2	2.29	2.83	3.86	0.619	0.64	0.864	21.36	23.36	21.95
6	42.9	43.1	43.2	194.7	199.9	199.5	18	20.9	18.6	33.7	39.8	43.3	3.23	3.94	4	0.29	0.52	0.55	34.5	35.56	36.2
7	69.7	70.3	70.9	135.2	140.1	147.8	9.4	13.5	16.2	18.1	26.6	29.3	1.54	1.6	2.4	1	1.66	2.1	33.5	41.42	48.78
Mean	55.3	56.1	56.6	177	178.8	196.6	9.3*	12.7	13.9	20*	28.1	31.8	2.22	2.75	3.84*	0.794*	1.029	1.287*	22.85†	24.19	26.07
SEM	5	4.7	4.8	11.5	12.2	10.6	1.7	1.7	1.7	2.7	2.6	2.9	0.32	0.33	0.59	0.113	0.179	0.224	3.36	4.03	4.74

*$p < 0.05$ versus control; †$p = 0.09$ versus control. All values are mean values ± SEM. A = inferior vena cava occlusion; B = control volume loading; C = calcium infusion. >220 = saturation of recorded data channel secondary to hypertension caused by intervention.

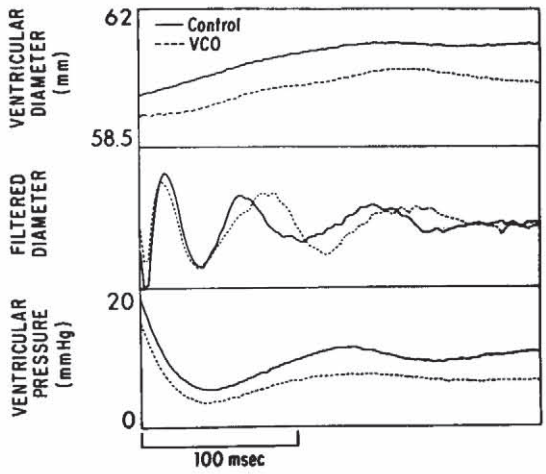

Figure 4. Superimposed high speed plots during rapid ventricular filling after phenylephrine infusion, volume loading and aortic occlusion (Control, **solid line**) and subsequent steady state inferior vena cava occlusion (VCO, **dashed line**) in a typical study. With the fall in filling pressure during vena caval occlusion, the frequency of wall oscillations decreased (**dashed line**, middle panel). Similar results were obtained in all seven dogs.

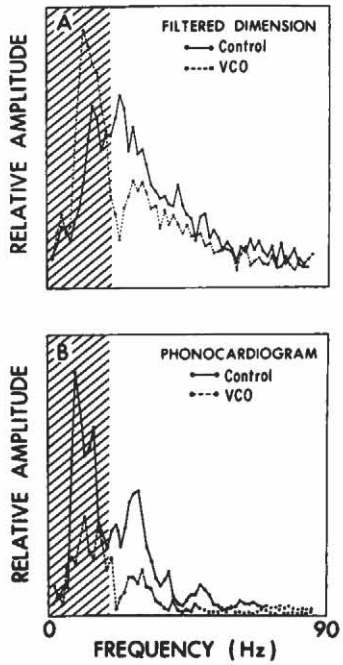

Figure 5. A, Fourier analysis of the filtered dimension data for six cardiac cycles during rapid ventricular filling in a typical study with varied filling pressure. **B,** Corresponding Fourier analysis of the phonocardiogram for the same cardiac cycles. Frequencies <20 Hz, shown here with **shading**, were considered inaudible. With higher filling pressure and wall stiffness during phenylephrine infusion, volume expansion and aortic occlusion (Control, **solid line**), the frequencies shifted to the right into the audible range and were reflected in the phonocardiogram by a similar increase in sound intensity in the audible frequencies as compared with vena caval occlusion (VCO, **dashed line**). Similar data were obtained in all dogs.

by both a decrease in the amplitude of left ventricular wall oscillations ($p < 0.05$) and a trend toward a decreased frequency of wall oscillation ($p = 0.09$).

Mechanical correlates of S_3 amplitude and frequency. Fourier analysis of the filtered minor-axis dimension and the phonocardiogram quantified the change in frequency of ventricular wall oscillations during the interventions (Fig. 5). With decreased filling pressure during vena caval occlusion, the total vibratory energy, represented by the area under the amplitude versus frequency curve, usually changed minimally; however, the amplitudes generally shifted to the left, so that less energy was present in the audible range above 20 Hz.

Infusion of calcium increased both the velocity of ventricular filling and the amplitude of wall oscillations, whereas diastolic pressures and oscillation frequency did not change significantly (Fig. 6 and Table 1). As the rate of diastolic filling increased, total vibratory energy (again represented by the area under the amplitude versus frequency curve) increased for both the filtered diameter and the phonocardiogram, whereas the fundamental frequencies remained approximately the same (Fig. 7). Throughout the studies, spectral analysis of the phonocardiographic data seemed to be somewhat limited by a greater amount of extraneous noise in the phonocardiographic signal as compared with the filtered diameter.

Multiple regression analysis demonstrated a strong correlation between the mean frequency of wall oscillations and both minimal ventricular diastolic pressure ($r = 0.60$, $p = 0.004$) and end-diastolic pressure ($r = 0.47$, $p = 0.03$) (Fig. 8). Higher diastolic pressures were uniformly related to higher mean vibratory frequencies. Similarly, the high mean amplitude of wall oscillations correlated strongly both with filling rate ($r = 0.80$, $p = 0.0001$) (Fig. 8) and to a lesser extent with end-diastolic diameter ($r = 0.46$, $p = 0.03$). With all of these relations, however, pure interactions could not be obtained in the biologic setting because both filling rate and pressure tended to change to some extent with all interventions (Fig. 8).

In examining Table 1, it should be noted that partial vena caval occlusion decreased left ventricular end-diastolic pressure, end-diastolic diameter, peak systolic pressure and minimal diastolic pressure only slightly despite the significant decrease in amplitude and frequency of S_3. These otherwise small changes were necessary because any significant decrease in left ventricular filling by full vena caval occlusion caused S_3 to not be detectable. Similarly, in an already distended ventricle, the effect of calcium was primarily to increase peak systolic pressure and mean filling rate without a large increase in end-diastolic diameter or pressure.

Discussion

Etiology of S_3. Shortly after Potain (1) attributed S_3 to sudden tensing of the ventricle during rapid ventricular

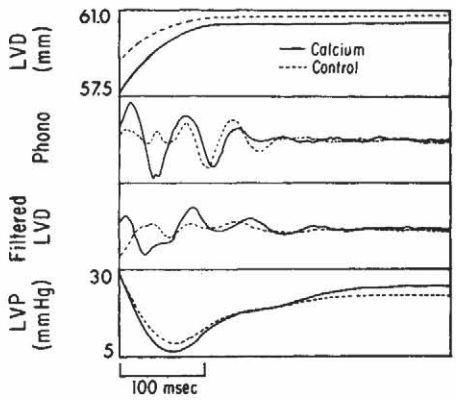

Figure 6. Superimposed high speed plots of left ventricular diameter (LVD), phonocardiogram (Phono), filtered diameter and left ventricular pressure (LVP) during rapid diastolic filling in a typical study. With increased filling rate demonstrated by the increased slope of the minor-axis diameter curve (Calcium, **solid line**), the amplitude of the rapid oscillations of the filtered diameter and phonocardiogram increased (**middle panels**) while the fundamental frequencies did not change significantly. Similar results were obtained in all dogs.

filling, alternative theories associated gallop sounds with the mitral valve apparatus (2–5). Although many investigators (2–5) have postulated that either tensing or closure of the mitral valve might produce an S_3, the role of valvular and

Figure 7. A, Average Fourier analysis of the filtered dimension for six cardiac cycles during rapid ventricular filling in a typical study under control conditions and during calcium infusion. **B,** Corresponding Fourier analysis of the phonocardiogram for the same cardiac cycles. The amplitudes of wall vibration increased significantly in both the phonocardiogram and filtered dimension with calcium infusion, while the fundamental frequencies were unchanged. Again, the inaudible frequencies (<20 Hz) are indicated with **shading.** Similar data were obtained in all dogs.

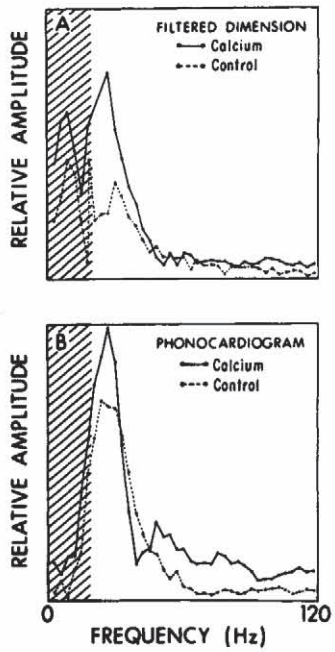

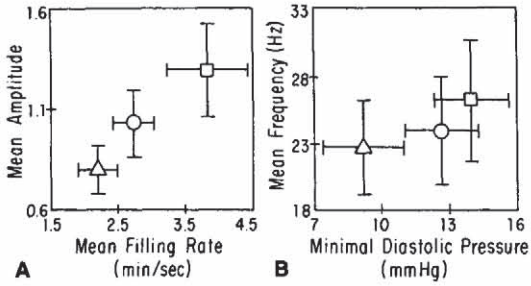

Figure 8. A, Relation between mean left ventricular filling rate and mean amplitude of ventricular wall vibrations for all seven experiments. **B,** Relation between left ventricular minimal diastolic pressure and mean frequency of ventricular vibrations for all seven experiments. **Open triangle** = vena caval occlusion; **open circle** = control; **open square** = calcium infusion.

subvalvular structures has been disputed by several clinical reports (23–25). In fact, S_3 gallop sounds have been observed in patients with an incompetent mitral valve heterograft (25), and patients have been described with a persistent S_3 after resection of both atrioventricular valves (23,24). Thus, available evidence suggests that the mitral apparatus contributes little to S_3.

In 1942, Boyer (6) proposed the theory that early diastolic motion of the heart caused an impact on the chest wall producing an S_3. Reddy et al. (7,8) noted that recordings of S_3 within the left ventricle were of lower amplitude than recordings of S_3 from the chest wall, thereby supporting the theory that S_3 results from impact of the left ventricle on the chest wall or from coupling of abrupt change in left ventricular velocity to the chest wall. Nonetheless, Craige et al. (12) dispute the theory of chest wall impact because they were able to record S_3 vibrations from the epicardial surface with the chest wall removed. Furthermore, other studies (13,14) demonstrated that S_3 vibrations were initiated with a marked deceleration (termed negative jerk) measured from both the epicardial surface and the chest wall, whereas Craige et al. (12) speculated that impact of the heart against the chest wall would produce an outward acceleration or positive jerk. Intracardiac pressure fluctuations also appear to be inadequate to account for the genesis of S_3 because an intracardiac S_3 may become apparent only during the terminal stages of heart failure, long after it is present by external cardiac recordings (8,12,13,26).

When the body of research concerning S_3 is reviewed in light of the present study, one may conclude that Potain (1) was correct in suggesting that S_3 is produced as the rapidly expanding ventricle reaches the point where the fibroelastic nature of the myocardium limits ventricular distension (9–16). The resulting sudden resistance to further chamber expansion under tension seems to generate a vibratory wave front that is detectable as a low frequency event by both the sonomicrometer and the phonocardiogram. Our data from the current experiments are consistent with this ventricular distension mechanism.

Mechanical correlates of S_3 amplitude and frequency. Despite general acceptance of the ventricular distension theory, data regarding the actual determinants of S_3 amplitude and frequency are limited to a few clinical studies. In children, Ewing et al. (15) found that S_3 energy <15 Hz decreased as filling velocity decreased with increased mitral valve orifice area, and they also observed that the high frequency component of S_3 increased with age (and possibly increased with ventricular stiffness). Porter et al. (27) noted that S_3 was most prominent in patients with increased peak ventricular filling rate or with increased wall stress at the time of peak left ventricular filling. Van de Werf et al. (28) noted that the presence of S_3 correlated with an increased rate of left ventricular filling (dV/dt) in patients with mitral regurgitation, and S_3 correlated with impaired left ventricular relaxation in patients with cardiomyopathy or constrictive pericarditis. Longhini et al. (16) demonstrated that the energy content of S_3 shifted toward higher frequencies in patients with increased ventricular wall thickness and decreased left ventricular diameter.

The current study supports the predictions of the ventricular distension theory with the frequency of S_3 influenced by ventricular diastolic pressure or wall stiffness and with the amplitude of S_3 determined by left ventricular filling rate (Fig. 8). These mechanical determinants of the third heart sound may be understood using a simple acoustic model of the left ventricle as an elastic sphere impacted by a mass of blood during ventricular filling, with resultant vibration in the left ventricular wall. The left ventricular wall would then be represented as a spring with elastic constant (k) and mass (m_{lv}), and the blood impacting the left ventricle during filling may be considered to have mass (m_b) and velocity (v_b). By conservation of momentum, the resultant initial velocity (v_{lv}) of displacement of the left ventricular wall would be related to the blood velocity (29)

$$v_{lv} = v_b\,(m_b/m_{lv})\,. \qquad [1]$$

The amplitude (A) of vibration of the wall will be (29)

$$A = v_{lv}\sqrt{m_{lv}/k}\,, \qquad [2]$$

or by substituting equation 1 into equation 2,

$$A = v_b\,(m_b/m_{lv})\,\sqrt{m_{lv}/k}\,. \qquad [3]$$

Thus, the amplitude of vibration will be roughly proportional to blood velocity (or rate of left ventricular filling) and *inversely* proportional to the square root of the left ventricular wall stiffness constant. Using this elastic spring model of the ventricular wall, the frequency of oscillation (f) would be (29)

$$2\pi f = \sqrt{k/m_{lv}}\,. \qquad [4]$$

If the left ventricle has significant dampening with dampening constant (c), the frequency of oscillation will be slightly reduced to (29)

$$2\pi f = \sqrt{(k/m_{lv}) - (c/2m_{lv})^2}\,. \qquad [5]$$

Note that the frequency of wall oscillation will be roughly proportional to the square root of the wall stiffness constant (k). Note also that, barring any change in wall stiffness, increased wall mass (as in left ventricular hypertrophy) may or may not produce an audible S_3 because S_3 frequency will decrease (equation 4) while S_3 amplitude increases (equation 2). Although modeling of the left ventricle as a linear spring and modeling of left ventricular filling as an impact between blood and the ventricular wall is clearly a simplification, the data presented in Table 1 and Figure 8 are consistent with such modeling.

Detection of S_3 by sonomicrometry. Sonomicrometry is well suited for studying wall oscillations related to S_3. This technique has maximal sensitivity to the most subtle ventricular vibrations over the frequency range of 0 to 250 Hz without the disadvantages of phonocardiography, which may pick up extraneous noises. Dynamic analysis of ventricular geometry and wall motion are possible with high resolution, stable electrical calibrations and negligible drift or temperature sensitivity. Additionally, the method is not hindered by the dampening effects of intervening tissues or extraneous noises that plague external monitoring techniques (20). Thus, sonomicrometry is ideal for the experimental application described in this study and could be extended to the clinical realm through intraoperative or postoperative studies of cardiac surgical patients (30).

Throughout the present study, results of sonomicrometry and phonocardiography were in agreement on the presence or absence of S_3 before and after volume loading and vena caval occlusion. Moreover, vibrations measured by epicardial sonomicrometry and S_3 measured by standard phonocardiography correlated both in amplitude and frequency over a range of ventricular filling rates and ventricular volumes and pressures (Fig. 3, 5 and 7). These correlations suggest that the vibrations measured by sonomicrometry did represent the S_3 detected by phonocardiography.

The studies of Ishimitsu et al. (31) suggested that the major axis of the ventricle played a more dominant role in the genesis of S_3 than did the minor axis. In a comparison of ventricular wall dynamics in both hyperdynamic and hypodynamic canine models, these authors noted that the peak major-axis dimensional velocity invariably was greater than the corresponding minor-axis velocity when an S_3 occurred. The diastolic differences between the minor and major axes are not surprising and are consistent with the anisotropic nature of the intact canine myocardium with greater stiffness in the major axis than in the minor axis (32). Although Ishimitsu et al. (31) noted better correlation between S_3 and deceleration in the major than in the minor axis, major- and minor-axis deceleration differed primarily in amplitude and not in their relation to S_3. The minor axis was chosen for investigation in our current study because of the relative facility of minor-axis transducer placement and because the changes in the minor axis with the appearance of an S_3 were sufficient to test the hypotheses outlined in the introduction.

JACC Vol. 19, No. 2
February 1992:450–7

Timing of S_3. In the current study (Fig. 3), S_3 followed relatively early after S_2 under control conditions. This relatively early timing of S_3 may have resulted from the high left ventricular filling rate produced by volume loading and elevated afterload in the control state. Earlier occurrence of S_3 with volume loading has been reported by Van de Werf et al. (33). In addition, the minor-axis diameter tracings of Figures 3, 4 and 6 might suggest that peak filling occurred slightly before the nadir in left ventricular pressure, while other investigators (9) have observed peak filling rates much closer to the ventricular pressure nadir. Much of the apparent discrepancy may result from minor-axis lengthening occurring earlier in diastole when the left ventricle is full (as in the present study) than when the ventricle is emptier (as in other studies) because of the more spheric shape of the full ventricle (22). In addition, the volume and pressure loading in the present study (mean left ventricular end-diastolic pressure 28 mmHg) might have caused the mitral valve to open prematurely, thus causing peak filling to occur before the nadir in left ventricular pressure.

Assessment of wall stiffness. One limitation of the current study was the indirect assessment of wall stiffness using diastolic left ventricular pressure, which could be more easily measured. Diastolic pressure, however, should be a reliable indicator of *changes* in wall stiffness because of the well defined exponential pressure-volume relation of the diastolic left ventricle (21) and because none of the interventions used to alter cardiac load or inotropic state affect the basic relation between left ventricular pressure and volume (and thereby pressure and stiffness) (21).

Because of the exponential pressure-volume relation of the left ventricle (21), an increase in ventricular diastolic pressure is associated with increased wall stiffness defined as the slope (dP/dV) of the pressure-volume relation. This increased wall stiffness would be expected to produce an increase in the frequency of ventricular vibrations for any given wall displacement induced by rapid filling (equation 4). A higher vibratory frequency would cause a corresponding shift of more acoustic energy into the audible range above 20 Hz, which might be perceived as S_3 becoming audible. In the intact heart, the relation between S_3 frequency and wall stiffness is supported by the observed rightward shift in frequency spectra of ventricular vibrations with increased filling pressure (Fig. 4 and 5, Table 1). The similar correlation between filling pressure and S_3 frequency observed with the external phonocardiogram in four dogs corroborates this observation (Fig. 4).

Assessment of ventricular filling rate. A second limitation of the present study was the use of left ventricular diameter to estimate relative left ventricular filling rate. Although Slinker and Glantz (34) demonstrated the potential inaccuracy of assessing instantaneous volume or rate of change in volume from left ventricular dimensions, left ventricular diameter was used in the present study only to detect *relative* changes in left ventricular filling rate. Other investigators have shown good correlation between change in ventricular volume and change in left ventricular dimensions (20,35), especially when high frequency resolution is not needed (34). Because the assessment of directional changes in mean rate of ventricular filling requires relatively low frequency information, the observations of Slinker and Glantz (34) are less relevant to the present study.

In these experiments, calcium was used to increase ventricular stroke volume in a volume-overloaded system while comparable diastolic pressures were maintained despite more efficient ventricular emptying. Because rapid ventricular filling intervals remained similar, mean filling rates increased (Fig. 6). At higher filling rates, the amplitude of wall vibrations increased significantly (Table 1, Fig. 8), but mean frequency changed little. Although it was impossible to vary filling rate or pressure in a completely independent fashion in the intact heart, the spectral data suggest that the amplitudes of S_3 and ventricular wall oscillations during rapid filling are proportional to the filling rate as predicted by equation 3. Higher filling rates would increase S_3 energy and could be perceived as an S_3 becoming audible.

Clinical implications for S_3 analysis. The observed relations between filling pressure, wall stiffness and the frequency of wall vibrations may have clinical relevance to the pathologic situations of congestive heart failure or ventricular hypertrophy, where an S_3 may become evident because of increased diastolic pressure or wall stiffness. The correlation between filling rate and amplitude of wall vibrations may have a clinical analog in high output states, such as thyrotoxicosis, or with lesions such as valvular incompetence that increase ventricular filling velocity. Finally, one might hypothesize that the development of an abnormal S_3 is dependent on an increase in either myocardial stiffness or rate of ventricular filling. Although similar principles might apply to the right ventricle, caution should be exercised in applying observations from the current study to a right ventricular third heart sound because the current study examined only the left ventricle.

It is reasonable to propose that different types of S_3 could be defined by spectral analysis of frequency and amplitude characteristics and that the data could be used for pathophysiologic interpretation of distinct clinical entities. Currently, the presence of an S_3 gallop plays a qualitative role in the management of patients with cardiac disorders (36–38) but spectral analysis could transform the phonocardiogram into a quantitative clinical tool. As Robert Hooke (39) so astutely stated in 1705, "Who knows, I say, but that it may be possible to discover the motions of the internal parts of the bodies . . . by the sound they make, that one may discover the works performed in several offices and shops of a man's body and thereby discover what instrument or engine is out of order."

We are grateful for the assistance of Louise Leighton in preparing the manuscript and of Joan Jones in preparing the illustrations.

References

1. Potain C. Les bruits de gallop. Semaine Med 1900;20:175–6.
2. Gibson AG. The significance of a hitherto undescribed wave in the jugular pulse. Lancet 1907;2:1380–2.
3. Thayer WS. Further observations on the third heart sound. Arch Intern Med 1909;4:297–305.
4. Dock W, Grandell F, Taubman F. The physiologic third heart sound: its mechanism and relation to protodiastolic gallop. Am Heart J 1955;50:449–64.
5. Flemming JS. Evidence for mitral valve origin of the left ventricular third heart sound. Br Heart J 1969;31:192–9.
6. Boyer NH. Studies on the third heart sound. Am Heart J 1942;23:797–802.
7. Reddy PS, Meno F, Curtiss EI, O'Toole JD. The genesis of gallop sounds: investigation by quantitative phono- and apexcardiography. Circulation 1981;63:922–32.
8. Reddy PS. The third heart sound. Int J Cardiol 1985;71:213–21.
9. Van de Werf F, Minten J, Carmeliet P, De Geest H, Kestlefoot H. The genesis of the third and fourth heart sounds. A pressure-flow study in dogs. J Clin Invest 1984;73:1400–7.
10. Kuo PT, Truman GS, Blakemore WS, Whereat AF. Diastolic gallop sounds, the mechanism of production. J Clin Invest 1957;36:1035–42.
11. Crevasse L, Wheat MW, Wilson JR, Leeds RF, Taylor WJ. The mechanism of generation of the third and fourth heart sounds. Circulation 1962;25:635–42.
12. Craige E, Ozawa Y, Smith D. Origin of the third heart sound. Acta Cardiol 1983;38:263–5.
13. Ozawa Y, Smith E, Craige E. Origin of the third heart sound. I. Studies in dogs. Circulation 1983;67:393–8.
14. Ozawa Y, Smith D, Craige E. Origin of the third heart sound. II. Studies in human subjects. Circulation 1983;67:399–404.
15. Ewing G, Mazumdar J, Goldblatt E, Fazzalari N, Van Vollenhoven E. A non-invasive study of the third heart sound in children by phono- and echocardiography. Acta Cardiol 1984;39:241–54.
16. Longhini C, Aggio S, Baracca E, Mele D, Fersini C, Aubert AE. A mass-spring model hypothesis of the genesis of the physiological third heart sound. Jpn Heart J 1980;30:265–73.
17. Olsen CO, Abert SJ, Glower DD, et al. A hermetically sealed cardiac dimension transducer for long-term animal implantation. Am J Physiol 1984;247:H857–60.
18. Vollenhoven EV, Beneken JEW, Reuver H, Dorenbos T. Filters for phonocardiography. Med Biol Eng 1967;5:127–38.
19. Olsen CO, Tyson GS, Maier GW, Davis JW, Van Trigt P, Rankin JS. Dynamic ventricular interaction in the conscious dog. Circ Res 1983;52:85–104.
20. Rankin JS, McHale PA, Arentzen CE, Ling D, Greenfield JC Jr, Anderson RW. The three-dimensional dynamic geometry of the left ventricle in the conscious dog. Circ Res 1976;39:304–13.
21. Rankin JS, Arentzen CE, Ring WS, Edwards CHII, McHale PA, Anderson RW. The diastolic mechanical properties of the intact left ventricle. Fed Proc 1980;39:141–7.
22. Olsen CO, Rankin JS, Arentzen CE, Ring WS, McHale PA, Anderson RW. The deformational characteristics of the left ventricle in the conscious dog. Circ Res 1981;49:843–55.
23. Towne WD, Crux J, Tatooles CJ, Chawala KK. Persistence of the third heart sound after resection of the native mitral and tricuspid valves. Chest 1976;70:100–2.
24. Coulshed N, Epstein EJ. Third heart sound after mitral valve replacement. Br Heart J 1972;34:301–8.
25. Gamal ME, Smith DR. Occurrence of a left ventricular third heart sound in incompetent mitral heterographs. Br Heart J 1970;32:497–500.
26. Aubert AE, Denys BG, Meno F, Reddy PS. Experimental study of intracardiac and external heart sounds by quantitative phonocardiography. Acta Cardiol 1983;38:292–4.
27. Porter CM, Baxley WA, Eddleman EE, Frimer M, Rackley CE. Left ventricular dimensions and dynamics of filling in patients with gallop heart sounds. Am J Med 1971;50:721–7.
28. Van de Werf F, Boel A, Geboers J, et al. Diastolic properties of the left ventricle in normal adults and in patients with third heart sounds. Circulation 1984;69:1070–8.
29. Burton R. Vibration and Impact. New York: Dover Publications, 1958: 17,50,110–2.
30. Tyson GS Jr, Olsen CO, Maier GW, et al. Dimensional characteristics of left ventricular function after coronary artery bypass grafting. Circulation 1982;66(suppl I):I-16–25.
31. Ishimitsu T, Smith D, Berko B, Craige E. Origin of the third heart sound: comparison of ventricular wall dynamics in hyperdynamic and hypodynamic states. J Am Coll Cardiol 1985;5:268–72.
32. Olsen CO, Glower DD, Lee KL, McHale PA, Rankin JS. Diastolic anisotropic properties of the left ventricle in the conscious dog. Circ Res 1991;69:765–78.
33. Van de Werf F, Minten J, Carmeliet P, DeGeest H, Kesteloot H. The genesis of the third and fourth heart sounds. A pressure-flow study in dogs. J Clin Invest 1984;73:1400–7.
34. Slinker BK, Glantz SA. The accuracy of inferring left ventricular volume from dimension depends on the frequency of information needed to answer a given question. Circ Res 1985;56:161–74.
35. Suga H, Sagawa K. Assessment of absolute volume from diameter of the intact canine left ventricular cavity. J Appl Physiol 1974;36:496–9.
36. Goldman L, Caldera DL, Nussbaum SR, et al. Multifactorial index of cardiac risk in noncardiac surgical procedures. N Engl J Med 1977;297:845–50.
37. Abdulla AM, Frank MJ, Erdin RA, Canedo MI. Clinical significance and hemodynamic correlates of the third heart sound gallop in aortic regurgitation. Circulation 1981;64:464–8.
38. Lee DC, Johnson RA, Bingham JB, et al. Heart failure in outpatients: a randomized trial of digoxin versus placebo. N Engl J Med 1982;306:699–705.
39. Hooke R. The present deficiency of natural philosophy is discoursed of, with the methods of rendering it more certain and beneficial. In Waller R. The Posthumous Works of Robert Hooke Containing his Cutlerian Lectures and Other Discources. London: Smith and Walford, 1705:39.